

# Inhibition of the NOTCH and mTOR pathways by nelfinavir as a novel treatment for T cell acute lymphoblastic leukemia

YOON SOO CHANG<sup>1\*</sup>, JOELL J. GILLS<sup>1,2\*</sup>, SHIGERU KAWABATA<sup>1-3</sup>, MASAHIRO ONOZAWA<sup>4</sup>, GIUSY DELLA GATTA<sup>5</sup>, ADOLFO A. FERRANDO<sup>5</sup>, PETER D. APLAN<sup>4</sup> and PHILLIP A. DENNIS<sup>1,2</sup>

<sup>1</sup>Medical Oncology Branch, Center for Cancer Research, National Cancer Institute, Bethesda, MD 20892;

<sup>2</sup>Department of Oncology, Johns Hopkins University School of Medicine, Baltimore, MD 21205, USA;

<sup>3</sup>Department of Pathology, Faculty of Medicine, Osaka Medical and Pharmaceutical University, Takatsuki, Osaka 569-8686, Japan; <sup>4</sup>Genetics Branch, Center for Cancer Research, National Cancer Institute, Bethesda, MD 20892;

<sup>5</sup>Institute for Cancer Genetics and Joint Centers for Systems Biology, Columbia University, New York, NY 10032, USA

Received February 12, 2023; Accepted September 1, 2023

DOI: 10.3892/ijo.2023.5576

**Abstract.** T cell acute lymphoblastic leukemia (T-ALL), a neoplasm derived from T cell lineage-committed lymphoblasts, is characterized by genetic alterations that result in activation of oncogenic transcription factors and the NOTCH1 pathway activation. The NOTCH is a transmembrane receptor protein activated by  $\gamma$ -secretase.  $\gamma$ -secretase inhibitors (GSIs) are a NOTCH-targeted therapy for T-ALL. However, their clinical application has not been successful due to adverse events (primarily gastrointestinal toxicity), limited efficacy, and drug resistance caused by several mechanisms, including activation of the AKT/mTOR pathway. Nelfinavir is a human immunodeficiency virus 1 aspartic protease inhibitor and has been repurposed as an anticancer drug. It acts by inducing endoplasmic reticulum (ER) stress and inhibiting the AKT/mTOR pathway. Thus, it was hypothesized that nelfinavir might inhibit the NOTCH pathway via  $\gamma$ -secretase inhibition and blockade of aspartic protease presenilin, which would make nelfinavir effective against NOTCH-associated T-ALL. The present study assessed the efficacy of nelfinavir against T-ALL cells and investigated mechanisms of action *in vitro* and in preclinical treatment studies using a *SCL-LMO1* transgenic mouse model. Nelfinavir blocks presenilin 1 processing and inhibits  $\gamma$ -secretase activity as well as the NOTCH1 pathway, thus suppressing T-ALL cell viability.

Additionally, microarray analysis of nelfinavir-treated T-ALL cells showed that nelfinavir upregulated mRNA levels of *CHAC1* (glutathione-specific  $\gamma$ -glutamylcyclotransferase 1, a negative regulator of NOTCH) and sestrin 2 (*SESN2*; a negative regulator of mTOR). As both factors are upregulated by ER stress, this confirmed that nelfinavir induced ER stress in T-ALL cells. Moreover, nelfinavir suppressed *NOTCH1* mRNA expression in microarray analyses. These findings suggest that nelfinavir inhibited the NOTCH1 pathway by downregulating *NOTCH1* mRNA expression, upregulating *CHAC1* and suppressing  $\gamma$ -secretase via presenilin 1 inhibition and the mTOR pathway by upregulating *SESN2* via ER stress induction. Further, nelfinavir exhibited therapeutic efficacy against T-ALL in an *SCL-LMO1* transgenic mouse model. Collectively, these findings highlight the potential of nelfinavir as a novel therapeutic candidate for treatment of patients with T-ALL.

## Introduction

T cell acute lymphoblastic leukemia (T-ALL) is a neoplasm derived from T cell lineage-committed lymphoblasts, accounting for ~15% of childhood and 25% of adult ALL cases. T-ALL affects bone marrow and peripheral blood, often presenting with a large thymic tumor, lymphadenopathy (tumor in lymph nodes) and hepatosplenomegaly (tumor in the liver and spleen). Thymic tumors are located in the anterior mediastinum and often exhibit rapid growth, which may manifest as respiratory distress caused by tracheal compression. T-ALL lymphoblasts have a scant cytoplasm (bare nucleus), express CD3, which is considered T cell lineage-specific, and frequently exhibit coexpression of CD4 and CD8 at the cortical T stage. Genetic alterations in T-ALL result in aberrant activities of oncogenic transcription factors and the NOTCH1 pathway, with del(9p) resulting in the loss of the tumor suppressor gene cyclin-dependent kinase inhibitor 2A (*CDKN2A*) (1,2).

Dysregulation of T cell-related transcription factors results from chromosomal rearrangements, including of T

---

*Correspondence to:* Dr Shigeru Kawabata, Department of Pathology, Faculty of Medicine, Osaka Medical and Pharmaceutical University, 2-7 Daigakumachi, Building C01, Fifth Floor, Takatsuki, Osaka 569-8686, Japan  
E-mail: shigeru.kawabata@ompu.ac.jp

\*Contributed equally

**Key words:** T cell acute lymphoblastic leukemia, nelfinavir, NOTCH pathway, mTOR pathway

cell receptor (TCR) genes. Oncogenic transcription factors implicated in T-ALL include T cell leukemia homeobox protein 1 (*TLX1*), *TLX3*, LIM domain only 1 (*LMO1*), *LMO2*, lymphoblastic leukemia-derived sequence 1 (*LYL1*) and T-ALL 1 (*TAL1*) (3,4). *TLX1* activation has been associated with a favorable prognosis in T-ALL, whereas the expression of *TAL1*, *LYL1* or *TLX3* has been associated with lower overall survival of patients with T-ALL (5). Genome-wide sequencing analyses in human T-ALL cohorts revealed associations between these oncogenic transcription factors and 10 pathways that are recurrently mutated in T-ALL, such as Myc, NOTCH and PI3K/AKT/mTOR (4,6). Taken together, the dysregulation of T cell-related transcription factors is implicated in T-ALL development and patient prognosis.

*TAL1* was originally identified as stem cell leukemia (*SCL*) gene arising from a translocation between chromosomes 1 and 14, t(1;14)(p33;q11), involving the regulatory element of the TCR gene in leukemic stem cells (7). *TAL1* protein requires either *LMO1* or *LMO2* for its oncogenic capacity (3). As previously reported (8), mice transgenic for full-length *SCL* alone do not develop T cell malignancy, whereas 19/20 (95%) of *SCL-LMO1* transgenic mice generated by crossing *sil-SCL* and *lck-LMO1* mice develop aggressive T cell leukemia/lymphoma by the age of 6 months. The immunophenotype and clinical manifestations of the disease in *SCL-LMO1* transgenic mice are similar to those observed in human patients with T-ALL. Tremblay *et al* (9) reported that *TAL1* and *LMO1* gain-of-function in *SCL-LMO1* transgenic mice precedes the acquisition of *Notch1* mutations for T-ALL initiation, suggesting that *SCL*, *LMO1* and *Notch1* gain-of-function may represent the minimum set of complementing events required for the transformation of susceptible thymocytes.

NOTCH is a transmembrane receptor for cell-cell communication that functions through three proteolytic cleavages. Briefly, NOTCH is produced in the endoplasmic reticulum (ER) as a single protein (pre-NOTCH), cleaved at its heterodimerization domain (HD) by a furin-like protease in the Golgi apparatus (S1 cleavage), indicating NOTCH maturation, then transported to the cell membrane as a transmembrane receptor comprising a heterodimer (mature form), including extracellular and intracellular NOTCH domains. Upon binding of a ligand, such as Jagged 1-2 or Delta-like ligands 1, 3 and 4, mature NOTCH undergoes two successive proteolytic cleavages (S2 and S3). S2 is mediated by a disintegrin and metalloproteinase. Finally, NOTCH is activated via S3 cleavage by  $\gamma$ -secretase, which is a hetero-tetrameric protein complex composed of one aspartic protease subunit, presenilin 1 or 2, and the three non-proteolytic subunits, namely, nicastrin, anterior pharynx defective-1 and presenilin enhancer protein 2 (10,11). Once NOTCH is recognized as a substrate of  $\gamma$ -secretase on the cytoplasmic membrane, presenilin undergoes endoproteolysis (endoproteolytic cleavage), termed autoproteolytic presenilin processing, to generate N- and C-terminal fragments (12-14), which results in the catalytic activation of  $\gamma$ -secretase for S3 cleavage at the transmembrane domain of the NOTCH receptor (10,15). Following S3 cleavage, the NOTCH intracellular domain translocates to the nucleus, resulting in induction of NOTCH target molecules, such as hairy and enhancer of split-1 (HES1) and c-Myc (11).

Mammals have four NOTCH receptors (NOTCH 1-4). Mutation frequencies for these vary between cancer types (11). *NOTCH1* gene is expressed in hematopoietic stem cells and controls several steps in thymocyte (T cell in the thymus) specification and differentiation (10,15,16). Somatic activating mutations of *NOTCH1* involving the extracellular HD in exons 26 and 27 and/or the C-terminal PEST domain consisting of a polypeptide enriched in proline (P), glutamic acid (E), serine (S) and threonine (T) in exon 34 have been identified in >50% of human T-ALL cases (17). Although *NOTCH1* activating mutations primarily occur in the HD and/or PEST domains, activating expansion mutations within the extracellular juxta-membrane domain (JM) in exon 28 have been identified in human T-ALL (18,19). By contrast, murine T-ALL is often associated with somatic deletions at the 5'-end of *NOTCH1*, resulting in ligand-independent Notch1 activation (20). These *NOTCH1* activating mutations in T-ALL suggest a potential role for inhibition of NOTCH1 pathway in cancer therapy.

$\gamma$ -secretase inhibitors (GSIs) are one of the most extensively studied NOTCH-targeting therapeutics to combat T-ALL (11,14). In early clinical trials of broad-spectrum GSIs, the maximum tolerable dose was limited by gastrointestinal toxicity (primarily diarrhea) resulting from intestinal secretory metaplasia, which was prevented by combination with glucocorticoid treatment (21,22). To date, the clinical application of GSIs to alleviate T-ALL has not been successful due to adverse events and limited anti-leukemic efficacy (11). It is reported that selective inhibition of  $\gamma$ -secretase components induces significant therapeutic efficacy and less toxicity in preclinical T-ALL models; MRK-560, a selective presenilin 1 inhibitor, suppresses leukemia development in both mutant *Notch1*-driven leukemia mouse models and human patient-derived xenograft (PDX) models, without any associated pathological changes in the gastrointestinal tract or major defects in thymocyte development (23,24). The mechanisms of resistance to NOTCH inhibition have been studied: Mutational loss of *PTEN*, a tumor suppressor gene, is a resistance mechanism in human T-ALL, which induces PI3K/AKT/mTOR pathway activity (25,26). For the successful clinical development of GSIs for T-ALL, selective targeting of presenilin 1 in  $\gamma$ -secretase and avoiding resistance to NOTCH inhibition by overcoming mechanisms such as PI3K/AKT/mTOR activation should be considered.

Our previous study demonstrated that nelfinavir, a human immunodeficiency virus 1 (HIV1) protease inhibitor, suppresses the proliferation of non-small cell lung cancer (NSCLC) cells *in vitro* as well as that of human NSCLC xenograft tumors by inhibiting AKT and inducing ER stress/unfolded protein response (UPR), which subsequently leads to apoptosis (27). Moreover, data from a phase I clinical trial of nelfinavir in adults with solid tumors shows that nelfinavir is well-tolerated and exhibits antitumor activity (28). More recently, we reported the antitumor effects of nelfinavir in a SCLC PDX mouse model. Nelfinavir increases levels of sestrin 2 (SESN2), an endogenous mTOR-negative regulator, via ER stress/UPR induction, resulting in inhibition of the mTOR pathway (29). To date, nelfinavir has been repurposed as an anticancer drug for various types of cancer such as lung, pancreas, head and neck carcinoma (30). Nelfinavir was originally developed to target

an HIV1 aspartic protease. Presenilin in  $\gamma$ -secretase is also an aspartic protease (31), therefore it was hypothesized that nelfinavir inhibits NOTCH pathway via  $\gamma$ -secretase inhibition by blocking presenilin, suggesting therapeutic efficacy against NOTCH-associated T-ALL. The present study, we assessed the efficacy of nelfinavir against T-ALL cells and investigated mechanisms of action *in vitro* and in preclinical treatment studies using a *SCL-LMO1* transgenic mouse model.

## Materials and methods

**Cell culture.** Jurkat and Molt4 cell lines were gifts from Dr David S Chervinsky (Roswell Park Memorial Institute, New York, NY, USA). HPB-ALL cell line was a gift from Dr A Thomas Look (Dana-Faber Cancer Institute, Boston, MA, USA), which was authenticated as previously described (32). The human T-ALL cell lines were maintained in RPMI-1640 medium supplemented with 5% fetal bovine serum (both Thermo Fisher Scientific, Inc.) at 37°C in an incubator with 5% CO<sub>2</sub>.

**Reagents.** Nelfinavir for *in vitro* experiments was obtained from the National Institutes of Health (NIH) AIDS Research and Reference Reagent Program, Division of AIDS, National Institute of Allergy and Infectious Diseases (Bethesda, MD, USA). Nelfinavir for *in vivo* experiments was obtained from Pfizer Inc. Compound E ( $\gamma$ -secretase inhibitor XXI; cat. no. 565790) and a fluorogenic  $\gamma$ -secretase substrate (cat. no. 565764) were purchased from Sigma-Aldrich (Merck KGaA). Rapamycin (an mTOR inhibitor) was obtained from LC Laboratories. Primary antibodies against cleaved NOTCH1 (Val1744; cat. no. D3B8; 1:1,000) for NOTCH1 intracellular domain (NICD), HES1 (cat. no. D6P2U; 1:1,000), c-Myc (cat. no. D84C12; 1:1,000),  $\alpha$ -tubulin (cat. no. 11H10; 1:1,000), presenilin 1 (cat. no. #3622; 1:1,000) to detect the full-length (FL) and C-terminal fragment (CTF),  $\beta$ -actin (cat. no. 13E5; 1:1,000), phosphorylated eukaryotic initiation factor 2 $\alpha$  (p-eIF2 $\alpha$ ; Ser51, cat. no. #3597; 1:1,000), NOTCH1 (cat. no. D6F11; 1:1,000) and p-S6 ribosomal protein (Ser235/236, cat. no. #2211; 1:1,000) were purchased from Cell Signaling Technology, Inc. ChaC glutathione-specific  $\gamma$ -glutamylcyclotransferase 1 (CHAC1; clone no. N116/14; 1:2,000) and CD3 (cat. no. #A0452; 1:100) antibodies were obtained from UC Davis/NIH NeuroMab Facility and Dako (Agilent Technologies, Inc.), respectively.

**Cell viability (apoptosis and cell death) assay.** T-ALL cells (2x10<sup>5</sup> cells per well) were plated in 6-well plates and treated with 1-20  $\mu$ M nelfinavir or an equal volume of 0.1% dimethyl sulfoxide (DMSO) for 16 h at 37°C. The cells were harvested and resuspended in fluorescein isothiocyanate (FITC)-labeled Annexin V in Binding Buffer (FITC Annexin V Apoptosis Detection kit I, BD Biosciences) for 15 min at room temperature and stained with 1 mg/ml propidium iodide (Sigma-Aldrich; Merck KGaA) in phosphate-buffered saline (PBS) at room temperature. Cells were immediately analyzed via flow cytometry. FACS analysis was performed using Becton-Dickinson and Company FACSsort and CellQuest software version 3.3 (BD Biosciences). FITC

Annexin V-positive staining was used to detect apoptosis (early + late phase). Propidium iodide was used to detect dead cells. Cells that were negative for both stains were considered viable.

**Immunoblotting analysis.** T-ALL cells (5x10<sup>5</sup> cells/well) were plated in 6-well plates, treated with nelfinavir, compound E, rapamycin or an equal volume of 0.1% DMSO at 37°C, then lysed in 2X lysis buffer [20% glycerol, 4% sodium dodecyl sulfate, 125 mM Tris-HCl pH 8.0] as previously described (33). Whole-cell protein lysate was quantified using a Pierce™ BCA Protein Assay kit (Thermo Fisher Scientific, Inc.). Afterward, 20  $\mu$ g lysate/lane was loaded and separated via 7.5-12.0% sodium dodecyl sulfate-polyacrylamide gel electrophoresis and transferred to nitrocellulose membranes. The membranes were blocked for 1 h at room temperature in blocking buffer [1X Tris-buffered saline (TBS), 5% milk and 0.1% Tween-20] and incubated with primary antibodies overnight at 4°C. Membranes were washed three times with wash buffer (1X TBS, 0.1% Tween-20). Primary antibodies were detected by incubation with horseradish peroxidase-linked secondary antibodies (anti-rabbit and -mouse IgG; cat. nos. #7074 and #7076, respectively; both 1:2,000; both Cell Signaling Technology, Inc.) for 1 h at room temperature and visualized using an enhanced chemiluminescence detection system (Amersham ECL detection reagent, cat. no. RPN2232, GE HealthCare). As loading controls,  $\alpha$ -tubulin or  $\beta$ -actin was used. Immunoblotting experiments were performed at least three times. Densitometry was performed using NIH Image software (version 1.52, National Institutes of Health).

**Cell-free *in vitro*  $\gamma$ -secretase assay.** Cytoplasmic membrane-enriched cell fractions were prepared using hypotonic buffer A (10 mM Tris pH 7.4, 1 mM EDTA and 1 mM EGTA) and dissolved in hypotonic buffer B (10 mM Tris pH 7.4, 1 mM EDTA, 1 mM EGTA and 0.2% CHAPS). To measure enzyme activity, 20  $\mu$ g protein was incubated with 8  $\mu$ mol/l fluorogenic  $\gamma$ -secretase substrate NMA-GGVVIATVK(DNP)-DRDRDR-NH<sub>2</sub>, nelfinavir or compound E for 2 h at 37°C. The degree of fluorogenic substrate cleavage was measured by emitted fluorescence using an Infinite 200 PRO microplate reader (Tecan Group, Ltd.) with an excitation wavelength of 355 nm and an emission wavelength of 440 nm, as previously reported (34,35).

**Microarray assay.** RNA was isolated from triplicate samples of 0.1% DMSO or 20 mM nelfinavir-treated HPB-ALL cells using TRIzol (Thermo Fisher Scientific, Inc.). cDNA was synthesized using SuperScript II Reverse Transcriptase (Thermo Fisher Scientific, Inc.) and processed for Affymetrix gene expression analysis (GeneChip Human Genome U133 Plus 2.0 Array, cat. no. 900466; GeneChip Scanner 3000; Affymetrix; Thermo Fisher Scientific, Inc.), following the manufacturer's instructions. Gene expression data were normalized using DNA-Chip-Analyzer software (softpedia.com/get/Science-CAD/dChip.shtml; dchip.org/; Build date: Jul 19 2010) and differentially expressed genes were identified using Comparative Marker Selection (version 8) GenePattern application (genepattern.org/#) using a non-parametric P<0.0001.

**Animal experiments.** *SCL-LMO1* transgenic mice that develop T cell malignancy were generated by crossing *sil-SCL* transgenic mice and *lck-LMO1* mice, as previously described (8). A total of ~300 mice (>14 weeks of age, 1:1 of males and females, 18 to 30 g of weight) were prepared and supplied from Genetics Branch, National Cancer Institute (NCI, Bethesda, MD) and maintained with *ad libitum* feeding and water and clean and comfortable environment (12-14/10-12 h dark cycle, 18-23°C with 40-60% humidity) in animal facility (NIH, Bethesda, MD, USA).

**Treatment with nelfinavir.** Measurable lesions, including thymic masses with or without peripheral lymphadenopathy, were screened using SkyScan1178 (Bruker Corporation) for whole-body X-ray and micro-computed tomography (CT) images under general anesthesia using isoflurane (3-4% for induction and 1-3% for maintenance) once/week. Once the measurable lesion was detected by imaging, mice with good physical condition were treated with intraperitoneal 100 mg/kg nelfinavir dissolved in vehicle (4% DMSO, 5% polyethylene glycol, 5% Tween-80 in saline) daily for 2 weeks, as previously described (29). Additionally, for nelfinavir-withdrawal study, four mice that had showed the efficacy of nelfinavir treatment were continuously administered vehicle until disease progression. The condition of mice was checked daily before and after nelfinavir treatment to monitor the progression of internal lesions once/week.

**Evaluation of nelfinavir efficacy.** Tumor burden (TB) was calculated based on the maximum tumor area of measurable lesions and the percentage of TB after nelfinavir treatment was calculated as ratio to TB before the treatment, which was indicated as 'TB (%) end'. Response rate (RR) was calculated based on the percent change in TB before and after nelfinavir treatment, as previously described (36): Complete response (CR), disappearance of all target lesions; partial response (PR),  $\geq 30\%$  decrease in target lesion; progressive disease (PD),  $\geq 20\%$  increase in target lesion and stable disease (SD),  $< 30\%$  decrease and  $< 20\%$  increase in target lesion. Baseline TB was used as a reference. Once RR was confirmed in nelfinavir treatment study, the mice were sacrificed. Additionally, mice with clinical signs such as hunched posture, rapid/progressive weight loss, or respiratory distress were prematurely sacrificed as a humane endpoint. Mice were euthanized by CO<sub>2</sub> asphyxiation with a volume displacement rate of 30-70% of the chamber volume/min based on the NIH Animal Research Advisory Committee Guidelines (<https://oacu.oir.nih.gov/animal-research-advisory-committee-arac-guidelines>) for euthanasia of rodents. Death after CO<sub>2</sub> asphyxiation was verified by lack of response to any stimulation.

To detect CD4+/CD8+ (double-positive) cell populations, single-cell suspensions from thymic tumor of *SCL-LMO1* transgenic mice were prepared. The cells were resuspended in calcium- and magnesium-free Hanks' balanced salt solution buffer (Thermo Fisher Scientific, Inc.) containing 2% fetal bovine serum and incubated for 30 min on ice with phycoerythrin-CD4 and FITC-CD8 (BD Pharmingen; BD Biosciences). The cells were washed twice with PBS and stained with 1 mg/ml propidium iodide in PBS at room temperature. FACS analysis was performed as aforementioned.

To perform hematoxylin and eosin (H&E), terminal deoxynucleotidyl transferase-mediated deoxyuridine triphosphate nick-end labeling (TUNEL) and CD3 immunohistochemical analysis, tissue pieces (thymus and bone marrow) from each mouse (Table SI) were dissected and fixed in 10% neutral buffered formalin for 24 h at room temperature, and then embedded in paraffin wax. The formaldehyde-fixed and paraffin-embedded (FFPE) tumor sections on glass slides were deparaffinized. Hematoxylin and eosin were stained for two minutes, respectively with rinsing using deionized water at room temperature, and then mountings were performed using Fisher Chemical™ Permount™ Mounting Medium (cat. no. SP15-100, Thermo Fisher Scientific, Inc.). FFPE tumor sections on glass slides were deparaffinized and hydrated, then stained with Apo-Direct TUNEL Assay kit (cat. no. 88-6611-88, Thermo Fisher Scientific, Inc.) according to the manufacturer's instruction. The glass slides were counter-stained with hematoxylin for 2 min at room temperature, visualized TUNEL-positive nuclei, and assessed on ten fields using a light microscopy as previously described (27). For CD3 immunohistochemical analysis, unstained FFPE tumor sections on glass slides were deparaffinized and hydrated, then stained with VECTASTAIN Elite ABC system (Vector Laboratories, Inc.; Maravai LifeSciences) according to the manufacturer's instruction, in which staining was performed using 3,3'-Diaminobenzidine (Sigma-Aldrich; Merck KGaA) at room temperature under monitoring the staining process using a light microscope, as previously described (36).

**Sequencing.** *Notch1* mutations in nelfinavir-treated *SCL-LMO1* transgenic mice were analyzed. For DNA preparation, tissue pieces (thymus, spleen, and bone marrow) from each mouse (Table SI) were dissected, flash-frozen and stored at -70°C until use. Tissue was chopped into <0.5 mm<sup>3</sup> pieces on dry ice and DNA was extracted using a Qiagen DNAeasy Blood & Tissue kit (Qiagen Inc.) according to the manufacturer's instructions. *Notch1* exons 26 and 27 (HD), exon 28 (JM) and exon 34 (PEST domain) were amplified from genomic DNA via PCR using the following primer sequences: Exon 26 forward, 5'-GCTGAGGGAGGACCTGAACCTGG-3' and reverse, 5'-CCTGAGCTGGAATGCTGCCTCTA-3'; exon 27 forward, 5'-CATGGGCCTCAGTGTCT-3' and reverse, 5'-TAGCAACTGGCACAAACAGC-3'; exon 28 forward, 5'-GCGTAGCCGCTGCCTGAT-3' and reverse, 5'-CAGACTCCCGGTGAGGATGC-3'; exon 34 forward 1, 5'-GCTGGCCTTTGAGACTGG-3' and reverse 1, 5'-CTCCTGGGCAGAATAGTGT-3'; exon 34 forward 2, 5'-ACAGATGCAGCAGACAGAAC-3' and reverse 2, 5'-CCTGGG GCCAGATAAACAGTACA-3'. PCR was performed as described by Sulis *et al.* (18) and analyzed using direct dideoxy Sanger sequencing of the PCR products in DNA Sequencing and Gene Expression Core (NCI). Somatic deletions at the 5'-end of *Notch1* were analyzed via PCR-based detection using the following primer sequences: Forward, 5'-ATGGTGGAA TGCCTACTTTGTA-3' and reverse, 5'-CGTTTGGGTAGA AGAGATGCTTTAC-3', as described by Ashworth *et al.* (20).

**Statistical analysis.** Data are presented as the mean  $\pm$  SD. The statistical significance of differences between treated and untreated cells was analyzed using one-way analysis of

variance followed by Bonferroni's post hoc test. All analyses were performed using the GraphPad Prism software version 9 (GraphPad Software Inc.; Dotmatics).  $P < 0.05$  was considered to indicate a statistically significant difference.

## Results

**Nelfinavir suppresses T-ALL cell viability.** To evaluate the cytotoxicity of nelfinavir in T-ALL cells, cell viability assay was performed. T-ALL cell lines with active NOTCH pathway that harbor either *NOTCH1* wild-type (Jurkat cells) or activating *NOTCH1* mutations (Molt4 and HPB-ALL cells) (17) were treated with 0.1% DMSO or nelfinavir. Nelfinavir decreased the percentage of viable cells in a dose-dependent manner compared with DMSO treatment in activating *NOTCH1* mutant T-ALL as well as in the wild-type cell line (Figs. 1 and S1). Although Molt4 cells showed a cell death plateau at high concentrations (10 and 20  $\mu\text{M}$ ), taken together, these findings suggested that nelfinavir might inhibit NOTCH activation in T-ALL cells.

**Nelfinavir inhibits the NOTCH1 pathway.** To assess whether nelfinavir inhibits NOTCH activation to exert its cytotoxic effects, NOTCH pathway activity in nelfinavir-treated T-ALL cells was evaluated. Following 16 h treatment, nelfinavir downregulated NICD expression in all cell lines at 5 and 10  $\mu\text{M}$  in a dose-dependent manner (Fig. 2). In addition, nelfinavir decreased expression of NOTCH1 target molecules (HES1 and c-Myc) at concentrations  $\geq 10 \mu\text{M}$ . Cell death-associated decomposition may affect the results of immunoblotting analyses after 16 h treatment; therefore, nelfinavir efficacy was assessed at earlier time points (Fig. S2). Nelfinavir downregulated expression of NICD and c-Myc in a time-dependent manner after 4 h treatment, indicating the efficacy of nelfinavir in the early phase. Taken together, these findings indicate that inhibition of the NOTCH1 pathway may underlie the cytotoxicity of nelfinavir against T-ALL.

**Nelfinavir inhibits  $\gamma$ -secretase activity.** To assess how nelfinavir inhibits the NOTCH1 pathway, cell-free *in vitro*  $\gamma$ -secretase assays were performed. When nelfinavir was added to membrane extracts isolated from Jurkat cells, relative fluorescence was inhibited by 40% at 10  $\mu\text{M}$  and 56% at 20  $\mu\text{M}$  (Fig. 3). These findings indicated that nelfinavir decreased fluorogenic substrate cleavage by endogenous  $\gamma$ -secretase, suggesting an inhibitory effect on  $\gamma$ -secretase activity. In addition, nelfinavir inhibited  $\gamma$ -secretase activity in membrane extract from HPB-ALL cells. Similar to compound E treatment as a positive control, nelfinavir inhibited  $\gamma$ -secretase activity in a dose-dependent manner after 2 h treatment, indicating that nelfinavir inhibited the NOTCH1 pathway via inhibition of  $\gamma$ -secretase activity.

**Nelfinavir blocks presenilin 1 processing.** To assess how nelfinavir inhibits  $\gamma$ -secretase activity, the effect of nelfinavir on presenilin processing was examined. T-ALL cells were treated with nelfinavir and full-length (FL) and the C-terminal fragment (CTF) of presenilin 1 were detected via immunoblotting (Fig. 4). Nelfinavir notably

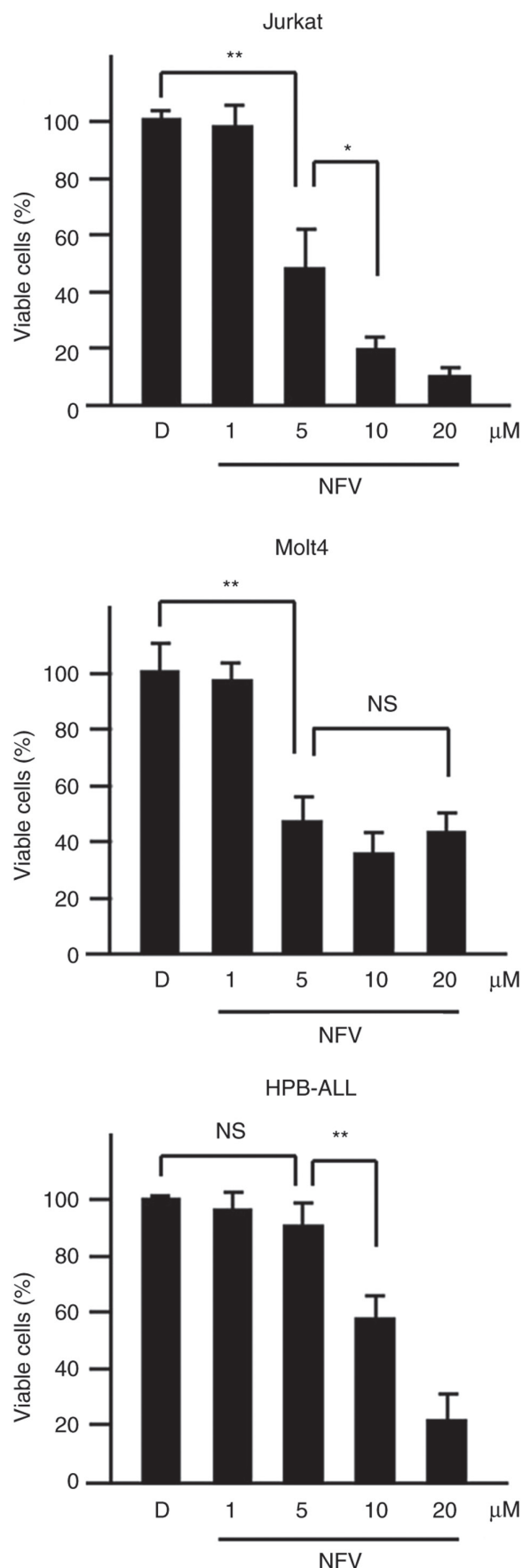


Figure 1. NFV suppresses T-ALL cell viability. T-ALL cells were treated with 0.1% D or NFV for 16 h. Cell viability assays were performed. Data are presented as the mean  $\pm$  SD of at least three separate experiments. \* $P < 0.05$ , \*\* $P < 0.01$ . NS, not significant; T-ALL, T cell acute lymphoblastic leukemia; NFV, nelfinavir; D, DMSO.

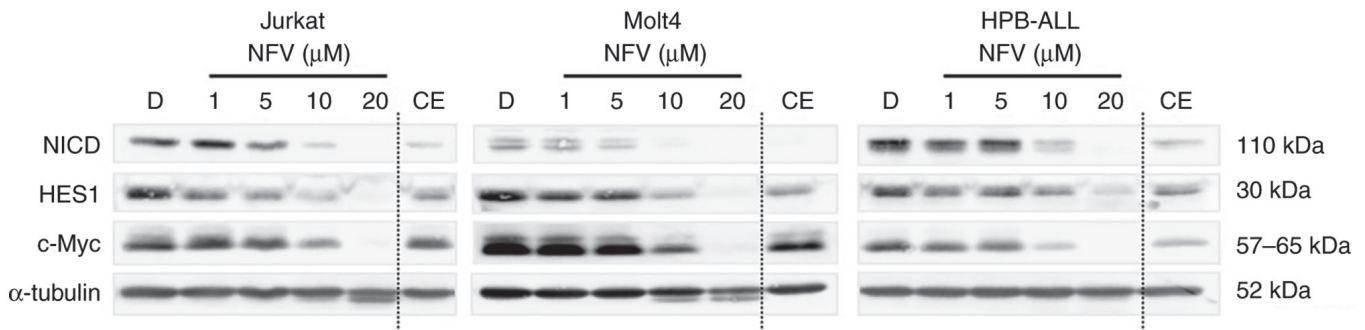


Figure 2. NFV inhibits the NOTCH1 pathway in a dose-dependent manner. T-ALL cells were treated with 0.1% D, NFV or 1  $\mu$ M CE for 16 h. Immunoblotting analyses were performed. CE was used as a control to confirm NOTCH1 inhibition. T-ALL, T cell acute lymphoblastic leukemia; NICD, NOTCH1 intracellular domain; HES1, hairy and enhancer of split-1; NFV, nelfinavir; D, DMSO; CE, compound E.

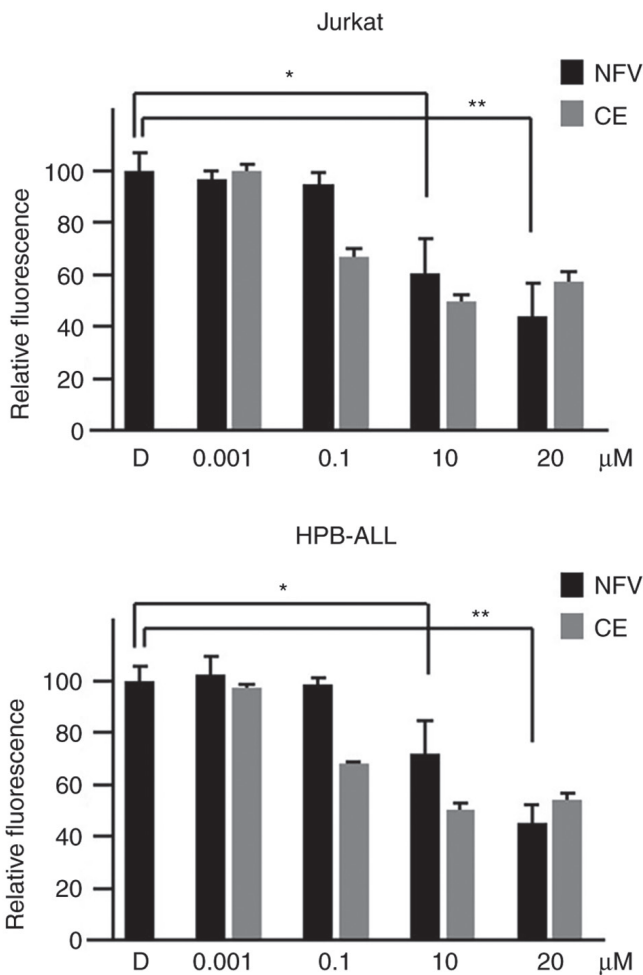


Figure 3. NFV inhibits  $\gamma$ -secretase activity in T-ALL cell lines. NFV decreased relative fluorescence in cell-free *in vitro*  $\gamma$ -secretase assay in a dose-dependent manner using cell membrane-enriched fractions. CE was used as a control to confirm specificity of fluorogenic substrate cleavage by endogenous  $\gamma$ -secretase. Data are the mean  $\pm$  SD of at least three separate experiments. \* $P$ <0.05, \*\* $P$ <0.01. T-ALL, T cell acute lymphoblastic leukemia; NFV, nelfinavir; D, DMSO; CE, compound E.

decreased expression of presenilin 1 CTF, suggesting that it blocked autoproteolytic processing of FL presenilin 1. Taken together, these findings suggested that nelfinavir inhibited  $\gamma$ -secretase activity by blocking presenilin 1 processing.

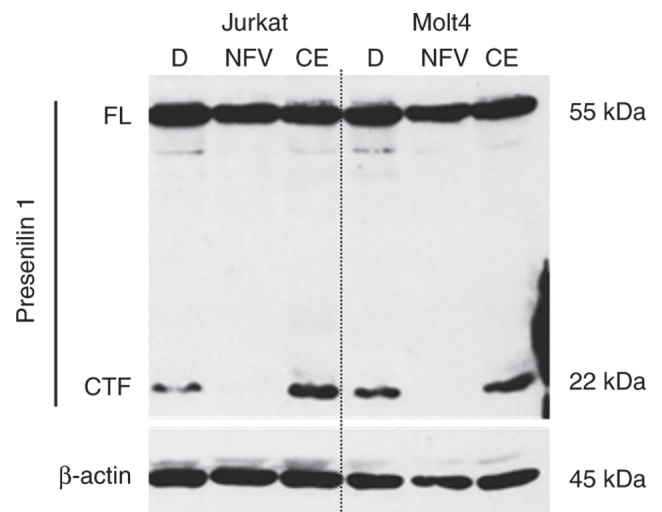


Figure 4. NFV blocks presenilin 1 processing. T-ALL cells were treated with 0.1% D, 20  $\mu$ M NFV or 1  $\mu$ M CE for 16 h. FL and CTF presenilin 1 levels were assessed using immunoblotting analysis. T-ALL, T cell acute lymphoblastic leukemia; NFV, nelfinavir; D, DMSO; CE, compound E; FL, full-length; CTF, C-terminal fragment.

*Nelfinavir increases CHAC1 expression and inhibits the mTOR pathway.* To determine the nelfinavir mechanism of action in T-ALL cells, HPB-ALL cells were treated with nelfinavir for 4 h before microarray assays. Among the top 50 differentially expressed genes, *HES* family members *HES1* and *HES4* were downregulated by nelfinavir compared with DMSO treatment (Fig. 5A). In addition, *NOTCH1* mRNA was moderately decreased by approximately 30%, along with downregulation of the NOTCH target gene *c-Myc* (Data S1). Nelfinavir upregulated *CHAC1* (Fig. 5A), a negative regulator of NOTCH that is induced by ER stress (37) and interferes with NOTCH maturation by blocking S1 cleavage, which results in NOTCH pathway inhibition (38). To assess whether *CHAC1* is involved in nelfinavir-induced NOTCH1 inhibition, immunoblotting analyses were performed for *CHAC1* as well as for FL, transmembrane, and NICD of NOTCH1 (Figs. 5B and S3A). In agreement with the microarray data, nelfinavir increased *CHAC1* expression in the three different cell lines. In addition, nelfinavir downregulated NICD, as well as the transmembrane and full-length forms of NOTCH1,

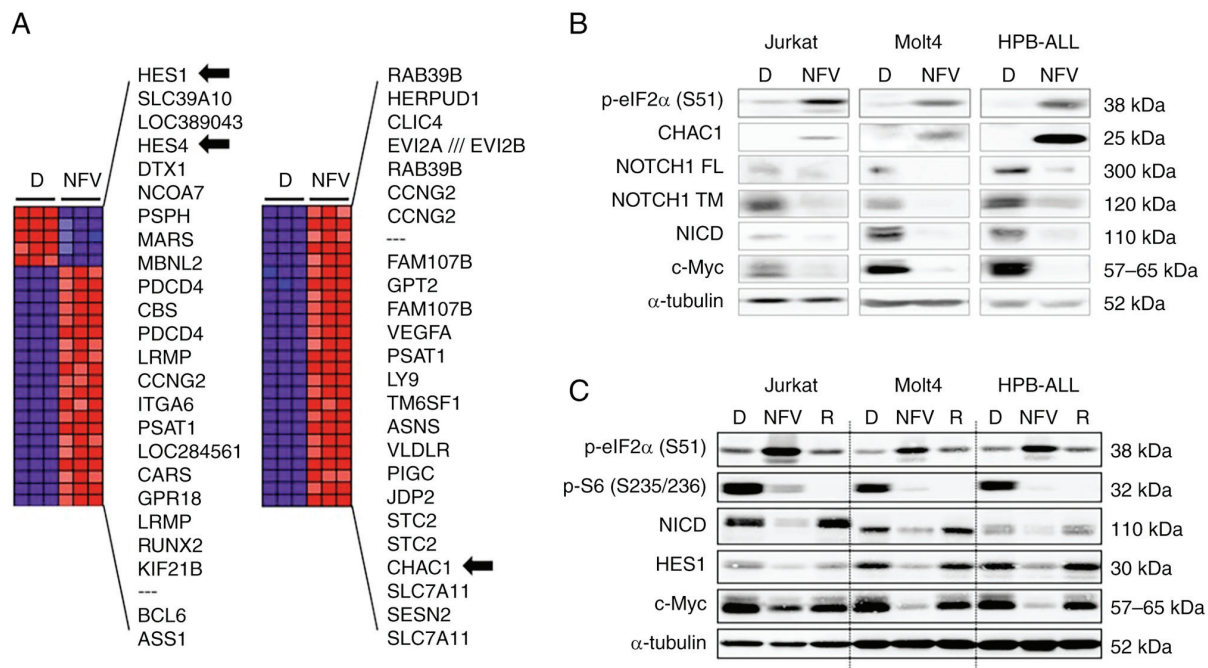


Figure 5. NFV increases CHAC1 expression and inhibits the mTOR pathway. (A) Expression changes induced by NFV. Top 50 differentially expressed genes in HPB-ALL cells treated with 20  $\mu$ M NFV for 4 h compared with 0.1% D treatment. Blue, relative decrease; red, relative increase; black arrow, NOTCH-related factors; SESN2, a negative regulator of mTOR. (B) T-ALL cells were treated with 0.1% D, 20  $\mu$ M NFV or (C) 100 nM R for 6 h to confirm inhibition of the mTOR pathway. Immunoblotting analyses were performed. CHAC1, ChaC glutathione-specific  $\gamma$ -glutamylcyclotransferase 1; HES1, hairy and enhancer of split-1; p-eIF2 $\alpha$  (S51), phosphorylated eukaryotic initiation factor 2  $\alpha$  subunit at Ser51; p-S6 (S235/236), phosphorylated S6 ribosomal protein at Ser235/236; FL, full-length; TM, transmembrane; NICD, NOTCH1 intracellular domain; T-ALL, T cell acute lymphoblastic leukemia; D, DMSO, NFV, nelfinavir; R, rapamycin; SESN2, sestrin 2.

suggesting that CHAC1 interferes with NOTCH1 maturation. Additionally, nelfinavir enhanced eIF2 $\alpha$  phosphorylation, indicative of ER stress induction. These findings suggest that nelfinavir inhibited the NOTCH1 pathway by inhibiting  $\gamma$ -secretase activity and interfering with NOTCH1 maturation through the upregulation of CHAC1 expression via ER stress induction.

Among the top 50 differentially expressed genes under nelfinavir treatment, negative mTOR regulator *SESN2* was upregulated by nelfinavir (Fig. 5A). To assess whether nelfinavir inhibited the mTOR pathway in T-ALL cell lines, immunoblotting analysis was performed for S6, which is an mTOR target (33). Nelfinavir decreased levels of phosphorylated S6, indicative of mTOR inhibition, and induced ER stress by enhancing levels of phosphorylated eIF2 $\alpha$  (Figs. 5C and S3B). These findings suggested that nelfinavir inhibited the mTOR pathway by increasing *SESN2* expression via the induction of ER stress.

#### *SCL-LMO1* transgenic mice develop T cell malignancy.

Given that *SCL-LMO1* transgenic mice that develop T cell malignancies have a high frequency of Notch1 activation due to acquisition of somatic *Notch1* mutations (8,39), these mice were used to evaluate the therapeutic potential of nelfinavir *in vivo*. The mice presented thymic tumors with or without peripheral lymphadenopathy between 14 and 25 weeks of age (Fig. 6A and B) and respiratory distress due to tracheal compression by the enlarged thymus. H&E staining showed no intact thymic tissue, whereas CD3-positive cells of T cell lineage proliferated diffusely (Fig. 6C and D). The proliferating

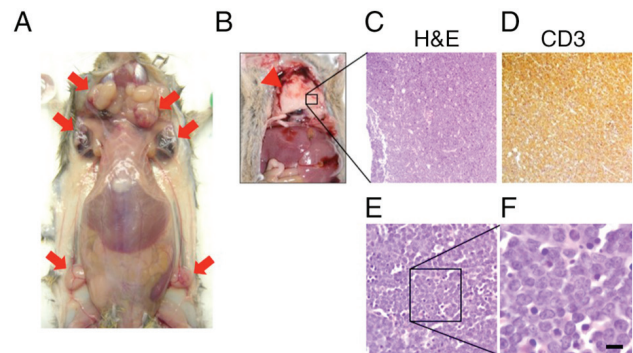


Figure 6. *SCL-LMO1* transgenic mice develop T cell malignancy. (A) General lymphadenopathy (tumor in lymph nodes) in a 21.1-week-old mouse. Red arrow, swollen lymph nodes. (B) Thymic tumor (red arrowhead) in a 24-week-old mouse. (C) H&E staining of the thymic tumor. (D) CD3 staining indicative of T cell lineage. Magnification, x100. (E) Thymic tumor exhibited lymphoblasts with a scant cytoplasm (high nuclear-cytoplasmic ratio). Magnification, x200. (F) Magnified inset (scale bar, 10  $\mu$ m). H&E, hematoxylin and eosin.

cells were lymphoblasts with scant cytoplasm, indicative of a high nuclear-cytoplasmic ratio (Fig. 6E and F). These T lymphoblastic cells were diffusely involved in the bone marrow and enlarged spleen, comprising 4-10% of leukocytes in the peripheral blood based on blood smear examination (data not shown). The immunophenotype of T lymphoblastic cells in the bone marrow, enlarged thymus and spleen exhibited CD4 and CD8 double-positive staining in flow cytometry analyses (data not shown). Collectively, these data supported

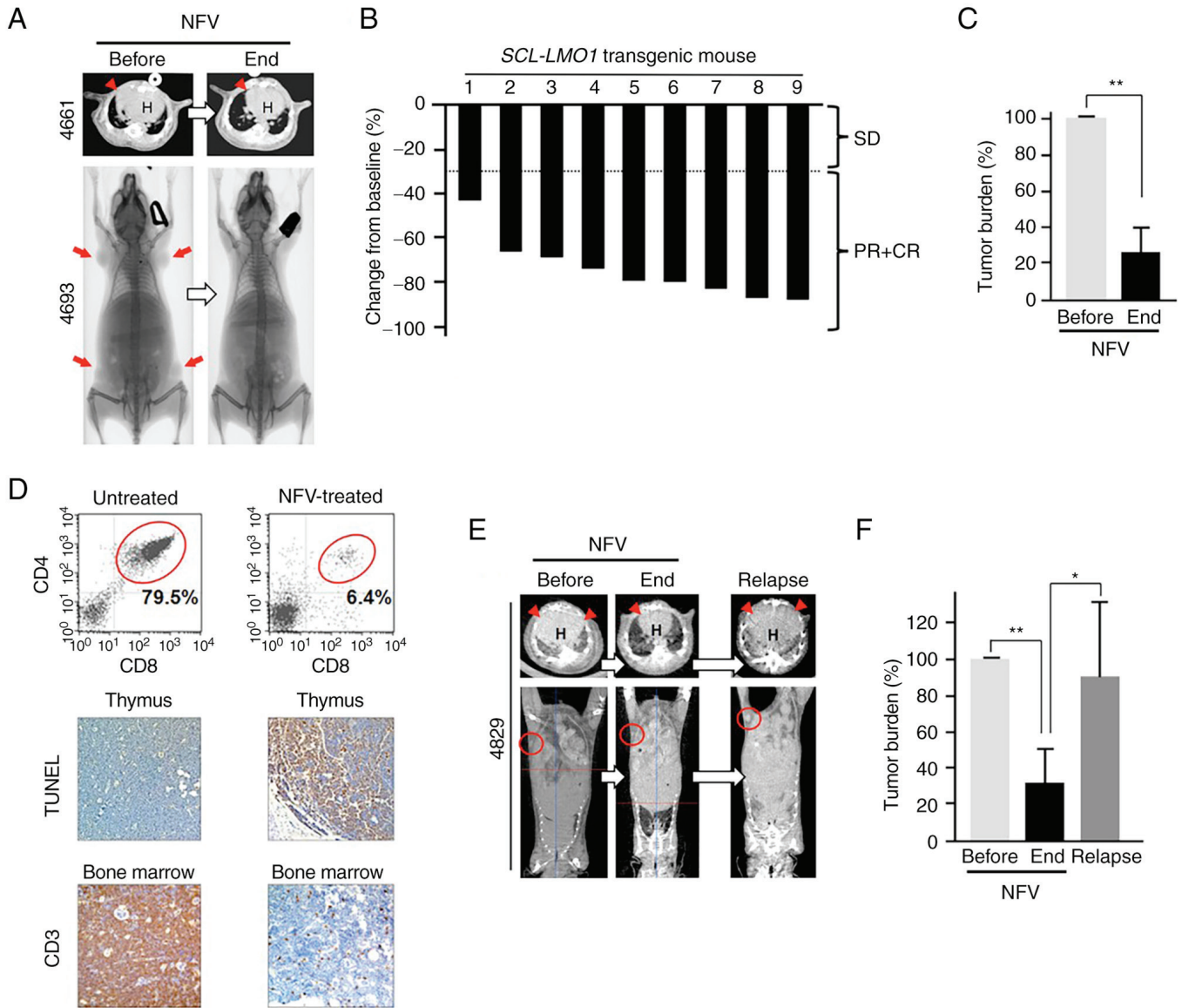


Figure 7. NfV decreases T cell malignant tumor burden in *SCL-LMO1* transgenic mice. (A) Representative micro-CT image of thymic tumor (red arrowhead) in mouse no. 4661 and whole-body X-ray of lymphadenopathy (tumor in lymph nodes, red arrow) in mouse no. 4693. Mice treated with 100 mg/kg NfV intraperitoneally daily for 2 weeks showed tumor regression. The mice were subjected to whole-body X-ray and micro-CT before and after NfV treatment. (B) Waterfall plot of change in tumor burden from baseline, based on response rate to NfV treatment. (C) NfV decreases tumor burden based on maximum tumor area in *SCL-LMO1* transgenic mice. (D) Efficacy of NfV treatment in *SCL-LMO1* transgenic mice. NfV treatment decreased CD4+/CD8+ (double-positive; red circle) tumor cells in the thymus compared with those in an untreated mouse, as per flow cytometry. Apoptosis of tumor cells in the thymus was increased by NfV treatment, as per TUNEL staining assay. CD3 staining showed population of T malignant tumor cells in the bone marrow decreased following NfV treatment. Magnification, x200. (E) NfV-withdrawal study in *SCL-LMO1* transgenic mice. Representative micro-CT images of mouse no. 4829 in panel. Treatment with 100 mg/kg NfV intraperitoneally daily for 2 weeks decreased tumor burden (red arrowhead, thymic tumor; red circle, lymphadenopathy indicating tumor in a lymph node). (F) NfV withdrawal induced tumor progression (relapse). \*P<0.05, \*\*P<0.01. H, heart; CR, complete response; PR, partial response; SD, stable disease; NfV, nelfinavir.

our previous findings (8) that *SCL-LMO1* transgenic mice develop T cell malignancies and are useful as a mouse model of human T-ALL.

*Nelfinavir decreases T cell malignant TB in SCL-LMO1 transgenic mice.* Mice were intermittently scanned by micro-CT from the age of 14 weeks to assess disease onset, defined by thymus enlargement with or without peripheral lymphadenopathy, prior to nelfinavir treatment. Nelfinavir treatment resulted in shrinkage of the thymic tumor and peripheral lymphadenopathy, indicating that malignant tumor cells (T lymphoblastic cells) were decreased (Fig. 7A). RR in

mice nos. 4661 and 4693 was 73.6 and 86.6%, respectively (Table SI). All nine mice treated with nelfinavir showed PR (Figs. 7B, S4 and S5; Table SI) and a 74% reduction in TB (Fig. 7C). Moreover, nelfinavir-treated mice showed a decrease in the number of CD4+/CD8+ tumor cells in the thymus as per flow cytometry analyses (Fig. 7D), in addition to more TUNEL-positive cells, indicative of tumor cell apoptosis enhanced by nelfinavir treatment. As shown by CD3 staining, malignant T cells in the bone marrow were decreased by nelfinavir treatment.

To confirm the efficacy of nelfinavir against T cell malignancy in *SCL-LMO1* transgenic mice, nelfinavir-withdrawal

study was performed. Treatment with 100 mg/kg nelfinavir for 2 weeks decreased TB in the thymus and peripheral lymph nodes, while nelfinavir withdrawal for 21 days induced tumor progression (Figs. 7E and S5). Mice treated with nelfinavir exhibited a mean 68% reduction in TB, whereas nelfinavir withdrawal induced tumor progression, indicating relapse (Fig. 7F; Table SII). Collectively, these findings indicated that nelfinavir exerted an antitumor effect against T-ALL *in vivo*.

*SCL-LMO1* transgenic mice develop T cell malignancies, with a frequency of *Notch1* mutations similar to that in humans (39). Therefore, to confirm an association between nelfinavir efficacy and *Notch* mutations, *Notch1* exons 26 and 27 (HD), 28 (JM) and 34 (PEST domain), as well as acquired somatic mutations at the 5' end, were sequenced in the tumors of treated mice. Sequencing showed that eight out of nine tissues had a PEST domain mutation; two out these also had a somatic deletion at the 5' end of *Notch1* (Table SI). Mutations in HD and JM were not detected. In total, *Notch1* mutations were detected in eight out of nine *SCL-LMO1* transgenic mice, indicating that these mice experience a physiological response to nelfinavir.

## Discussion

The present data showed that nelfinavir blocked presenilin 1 processing and activity of  $\gamma$ -secretase, thus blocking S3 cleavage, resulting in inhibition of NOTCH1 signaling and suppression of T-ALL cell viability. These findings support the hypothesis that nelfinavir suppresses the NOTCH pathway via  $\gamma$ -secretase inhibition, specifically by blocking presenilin, which may render it effective against NOTCH-associated T-ALL. Microarray assays revealed that nelfinavir upregulated *CHAC1*, which interfered with NOTCH1 maturation by blocking S1 cleavage. In addition, nelfinavir downregulated *NOTCH1* mRNA expression. Taken together, these findings suggested that nelfinavir inhibited the NOTCH1 pathway through multiple mechanisms, including suppression of *NOTCH1* gene expression, upregulation of *CHAC1* expression to interfere with NOTCH1 maturation and  $\gamma$ -secretase inhibition by blocking presenilin 1 processing (Fig. 8).

To the best of our knowledge, the present study is the first to describe that nelfinavir, as an HIV1 aspartic protease inhibitor, inhibits human aspartic protease presenilin 1, resulting in NOTCH1 pathway blockade. Aspartic proteases are divided into five superfamilies (clans): AA, AC, AD, AE and AF. Clan AA includes the HIV protease and classical aspartic peptidases, such as renin, pepsin and cathepsin, whereas clan AD includes intramembrane-cleaving proteases, such as presenilin and signal peptide peptidase (31,40). Recently, Gu *et al* (41) reported that nelfinavir inhibits human aspartic protease DNA damage-inducible 1 homolog 2 (DDI2), which belongs to Clan AA. Human DDI2 has a retroviral protease-like domain that is highly conserved in HIV protease, which results in the direct binding of nelfinavir to the domain for inhibition of DDI2 activity (41). It remains unclear whether presenilin has a retroviral protease-like domain (42,43) and whether nelfinavir could directly bind to presenilin remains to be solved. Here, nelfinavir notably decreased the expression of the CTF of

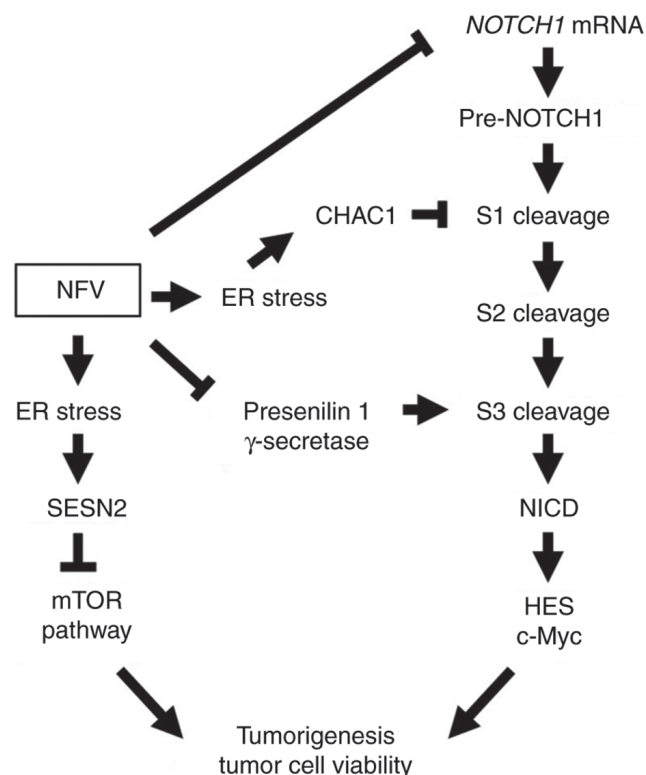


Figure 8. NFV inhibits the NOTCH1 pathway by downregulating *NOTCH1* mRNA, interfering with NOTCH1 maturation, wherein S1 cleavage is blocked by increasing *CHAC1* expression via ER stress induction, and  $\gamma$ -secretase inhibition through blockade of presenilin 1 processing, resulting in blocked S3 cleavage. NFV inhibits the mTOR pathway by increasing *SESN2* expression via ER stress induction. ER, endoplasmic reticulum; *CHAC1*, ChaC glutathione-specific  $\gamma$ -glutamylcyclotransferase 1; NICD, NOTCH1 intracellular domain; HES, hairy and enhancer of split; *SESN2*, sestrin 2; NFV, nelfinavir.

presenilin 1, which indicated inhibition of presenilin 1 activity as an aspartic protease, because CTF is essential for presenilin 1 activation (13). Endoproteolytic cleavage of CTF is mediated by the hydrophobic domain encoded by exon 9 of presenilin 1 (44). Nelfinavir-induced downregulation of CTF may be attributed to the inhibition of presenilin 1 endoproteolytic cleavage. Presenilinase is the enzyme responsible for endoproteolytic cleavage of presenilin. Current evidence suggests that presenilinase is presenilin, making presenilin endoproteolysis an autocleavage event (45). Further studies are needed to identify the nelfinavir mechanism responsible for CTF downregulation. Taken together, the aforementioned studies demonstrate that nelfinavir inhibits presenilin 1 activity for  $\gamma$ -secretase inhibition by blocking presenilin 1 processing via CTF downregulation, rather than by directly binding to the catalytic domain of presenilin 1.

Presenilin is an intramembrane-cleaving protease, with homologous polytopic proteins presenilin 1 and presenilin 2 forming the presenilin 1- or presenilin 2-containing  $\gamma$ -secretase complexes, respectively (46). In a previous study using presenilin-wild-type and knockout mouse embryonic fibroblasts (MEFs), presenilin 1, 2 or presenilin 1 and 2 double (-/-) MEFs were treated with EDTA to induce ligand-independent Notch activation (47), showing that presenilin 1 serves a key role in Notch1 activation. The presenilin 1-containing

$\gamma$ -secretase complex is primarily localized in the cytoplasmic membrane, whereas the presenilin 2-containing complex localizes to a greater extent at endosomes and lysosomes, including the trans-Golgi network (48). Moreover, the murine presenilin 1-containing  $\gamma$ -secretase complex serves a greater role in Notch activation compared with the presenilin 2-containing complex (49). The aforementioned findings suggest that presenilin 1 is a more important target molecule for Notch inhibition than presenilin 2. The present study performed cell-free *in vitro*  $\gamma$ -secretase assays by preparing cytoplasmic membrane-enriched cell fractions and showed that nelfinavir decreased cleavage of fluorogenic substrates by endogenous  $\gamma$ -secretase. However, the extent to which presenilin 1 was present in the endogenous  $\gamma$ -secretase complex was not determined, which is a limitation of the present study. Nonetheless, given that the presenilin 1-containing  $\gamma$ -secretase complex is primarily localized in the cytoplasmic membrane (48), presenilin 1 plays a major role in Notch1 activation and nelfinavir inhibits presenilin 1 activity by downregulating CTF, it is hypothesized that nelfinavir inhibits  $\gamma$ -secretase activity by inhibiting presenilin 1 rather than presenilin 2 activity. MRK-560 experiments suggest that presenilin 1-selective inhibition is a potential therapeutic strategy for safe and effective targeting of T-ALL (24). Taken together, nelfinavir may inhibit  $\gamma$ -secretase activity with less gastrointestinal toxicity than broad-spectrum GSI.

Microarray analysis showed that nelfinavir enhanced *CHAC1* gene expression. CHAC1 is a proapoptotic protein that is upregulated via the eIF2 $\alpha$ /activating transcription factor (ATF) 4/ATF3/C/EBP homologous protein pathway during ER stress (50) and functions as a  $\gamma$ -glutamyl cyclotransferase (GGCT) to degrade glutathione (51). Chi *et al.* (38) reported that CHAC1 inhibits the NOTCH1 pathway by serving as a GGCT to remove glycine from a  $\gamma$ -carbon-modified glutamate at position 1,669 of NOTCH1, resulting in blockade of S1 cleavage by furin-like protease in the Golgi apparatus. This interferes with NOTCH1 maturation, leading to lower cell surface expression of FL NOTCH1. Therefore, CHAC1 is also named blocker of NOTCH (38,52). Here, nelfinavir induced ER stress, as indicated by upregulation of phosphorylated eIF2 $\alpha$  and CHAC1 expression and downregulated NICD, suggesting that nelfinavir inhibited the NOTCH1 pathway by interfering with NOTCH1 maturation through increased CHAC1 following ER stress induction. Conversely, nelfinavir decreased the transmembrane and FL forms of NOTCH1 in T-ALL cells. The present study did not confirm whether nelfinavir decreases cell surface expression of FL NOTCH1. Microarray analysis showed that nelfinavir moderately decreased *NOTCH1* mRNA, suggesting that nelfinavir may interfere with NOTCH1 transcription, resulting in a decrease in the levels of both transmembrane and FL forms. Taken together, nelfinavir increases CHAC1 expression to interfere with NOTCH1 maturation by blocking S1 cleavage and decreasing *NOTCH1* mRNA expression, resulting in NOTCH1 pathway inhibition.

Microarray showed that nelfinavir upregulated *SESN2* gene expression, suggesting that nelfinavir may inhibit the mTOR pathway in T-ALL cells. mTOR is the catalytic subunit of mTOR complex 1 (mTORC1) and mTORC2. mTORC1 is activated via the PI3K/AKT/mTOR pathway to phosphorylate downstream target molecules, such as S6, promoting cell proliferation. By contrast, mTORC2 directly phosphorylates

AKT at Ser473, indicative of a feedback loop between AKT, mTORC1 and mTORC2 (53,54). *SESN2* is a stress-responsive gene, also known as hypoxia-induced gene 95 (55), which shares considerable homology with p53-regulated GADD family member *PA26* (56) and was named after the Italian town Sestri Levante (57). *SESN2* is upregulated by ER stress induction (58) and inhibits mTORC1 activation via upregulation of nutrient-responsive AMPK and modulation of GAP activity toward Rags 2 (GATOR2). Both AMPK and GATOR2 negatively regulate the mTORC1 pathway (59). Here, nelfinavir decreased phosphorylated S6 expression, indicating mTORC1 inhibition, which suggests that nelfinavir inhibited the mTOR pathway by upregulating *SESN2* through ER stress induction in T-ALL cells. These findings are supported by reports in other malignancies, such as breast and ovarian cancer and SCLC (29,60). As the PI3K/AKT/mTOR pathway is involved in mechanisms of resistance to NOTCH inhibition in T-ALL (25,26), nelfinavir may be cytotoxic to T-ALL cells via NOTCH1 inhibition and suppression of the mTOR-mediated resistance.

Nelfinavir decreased the T cell malignant TB in *SCL-LMO1* transgenic mice with *Notch1* mutation, indicating that nelfinavir might have therapeutic potential for NOTCH-associated human T-ALL. The present *in vivo* study had several limitations. First, the present study did not include a control cohort of mice treated with mock/vehicle. Measurable lesions (thymic masses, with or without peripheral lymphadenopathy) were screened via micro-CT. Once the lesion was detected, nelfinavir treatment was started as soon as possible since the mouse would die from respiratory distress caused by tracheal compression unless effective treatment were provided. The present study compared TB before and after nelfinavir treatment. Second, the present study did not evaluate the mechanisms of action by which nelfinavir decreased TB because residual tumors following nelfinavir treatment were used for *Notch1* mutation analyses and immunophenotype evaluation. Further studies of *in vivo* pharmacodynamics are needed to confirm nelfinavir mechanisms of action. Third, one (mouse no. 4661) nelfinavir-treated mouse experienced diarrhea on day 11 of nelfinavir treatment; however, the present study did not assess the possibility of gastrointestinal toxicity following Notch inhibition based on gastrointestinal tissue specimens. However, the other mice did not exhibit any gastrointestinal toxicity, indicating that nelfinavir may selectively target  $\gamma$ -secretase, as in the case of the presenilin 1-specific inhibitor MRK-560 (24). Taken together, the present *in vivo* study using *SCL-LMO1* transgenic mice supported the potential of nelfinavir against T-ALL.

F-box and WD repeat domain containing 7 (FBW7) is a ubiquitin ligase that plays a role in processes such as cell cycle progression and signal transduction through ubiquitination and degradation of its substrates, such as NOTCH and mTOR, suggesting a key role in both NOTCH and mTOR pathways (61,62). The present study confirmed that nelfinavir inhibited both pathways in an FBW7-independent manner using *FBW7* knockout DLD1 colorectal cancer cells (data not shown). ER stress induced by nelfinavir may underlie NOTCH and mTOR pathway inhibition via the upregulation of CHAC1 and *SESN2*. Collectively, the present findings highlight the potential of nelfinavir as novel therapeutics requiring further validation in T-ALL clinical trials.

## Acknowledgements

The authors would like to thank Mr Juan Morales Contreras, Mr Dumas Tarra and Dr John U Dennis (Laboratory Animal Medicine, NCI, Bethesda, MD, USA) for veterinary services and Ms Danielle Donahue (Mouse Imaging Facility, National Institute of Neurological Disorders and Stroke, NIH) for technical assistance with mouse whole-body X-ray and micro-CT scans. The abstract was presented at the 102nd annual meeting of the American Association of Cancer Research [2011 Apr 2-6, Orlando, Florida, USA; Cancer Res 2011;71(8 Suppl):Abstract nr 2603].

## Funding

The present study was supported by the Intramural Research Program of the NIH, Center for Cancer Research, NCI (grant no. ZIA SC 010378), Johns Hopkins University School of Medicine and Japan Society for the Promotion of Science KAKENHI (grant no. JP20K07646).

## Availability of data and materials

The datasets generated and/or analyzed during the current study are available in the Figshare repository, figshare.com/(accession no. 10.6084/m9.figshare.24061842).

## Authors' contributions

YSC, JJG and SK designed and performed experiments, analyzed and interpreted data and wrote the manuscript. MO performed *in vivo* experiments and analyzed and interpreted data. GDG performed, analyzed and interpreted the microarray experiments. AAF supervised the microarray experiments and interpreted data. PDA provided *SCL-LMO1* transgenic mice and interpreted *in vivo* data. PAD conceived and supervised the study. All authors have read and approved the final manuscript. YSC and SK confirm the authenticity of all the raw data.

## Ethics approval and consent to participate

*In vivo* experiments were approved by the NCI-Bethesda Animal Care and Use Committee (approval no. CTB-008, Bethesda, MD, USA).

## Patient consent for publication

Not applicable.

## Competing interests

The authors declare that they have no competing interests.

## References

- Borowitz MJ, Chan JKC, Béné M and Arber DA: T-lymphoblastic leukemia/lymphoma. In: WHO Classification of Tumours of Haematopoietic and Lymphoid Tissues (Revised 4th edition). Swerdlow SH, Campo E, Harris NL, Jaffe ES, Pileri SA, Stein H and Thiele J (eds) The International Agency for Research on Cancer, Lyon, pp209-213, 2017.
- Czader M, Molina TJ, Choi JK, Leventaki V, Miles RR, Lin P, Saha V, Tembhare P and Chandy M: T-lymphoblastic leukaemia/lymphoma, NOS. In: WHO Classification of Tumours Editorial Board. Haematolymphoid tumours [Internet; beta version ahead of print]. Vol 11. 5th edition. International Agency for Research on Cancer, Lyon, 2022. <https://tumourclassification.iarc.who.int/chapters/63>. Accessed January 17, 2023.
- Tan TK, Zhang C and Sanda T: Oncogenic transcriptional program driven by TAL1 in T-cell acute lymphoblastic leukemia. *Int J Hematol* 109: 5-17, 2019.
- Bardelli V, Arniani S, Pierini V, Di Giacomo D, Pierini T, Gorello P, Mecucci C and La Starza R: T-cell acute lymphoblastic leukemia: Biomarkers and their clinical usefulness. *Genes (Basel)* 12: 1118, 2021.
- Ferrando AA, Neuberg DS, Staunton J, Loh ML, Huard C, Raimondi SC, Behm FG, Pui CH, Downing JR, Gilliland DG, *et al*: Gene expression signatures define novel oncogenic pathways in T cell acute lymphoblastic leukemia. *Cancer Cell* 1: 75-87, 2002.
- Liu Y, Easton J, Shao Y, Maciaszek J, Wang Z, Wilkinson MR, McCastlain K, Edmonson M, Pounds SB, Shi L, *et al*: The genomic landscape of pediatric and young adult T-lineage acute lymphoblastic leukemia. *Nat Genet* 49: 1211-1218, 2017.
- Begley CG, Aplan PD, Davey MP, Nakahara K, Tchorz K, Kurtzberg J, Hershfield MS, Haynes BF, Cohen DI, Waldmann TA, *et al*: Chromosomal translocation in a human leukemic stem-cell line disrupts the T-cell antigen receptor delta-chain diversity region and results in a previously unreported fusion transcript. *Proc Natl Acad Sci USA* 86: 2031-2035, 1989.
- Aplan PD, Jones CA, Chervinsky DS, Zhao X, Ellsworth M, Wu C, McGuire EA and Gross KW: An scl gene product lacking the transactivation domain induces bony abnormalities and cooperates with LMO1 to generate T-cell malignancies in transgenic mice. *EMBO J* 16: 2408-2419, 1997.
- Tremblay M, Tremblay CS, Herblot S, Aplan PD, Hébert J, Perreault C and Hoang T: Modeling T-cell acute lymphoblastic leukemia induced by the SCL and LMO1 oncogenes. *Genes Dev* 24: 1093-1105, 2010.
- Grabher C, von Boehmer H and Look AT: Notch 1 activation in the molecular pathogenesis of T-cell acute lymphoblastic leukaemia. *Nat Rev Cancer* 6: 347-359, 2006.
- Zhou B, Lin W, Long Y, Yang Y, Zhang H, Wu K and Chu Q: Notch signaling pathway: Architecture, disease, and therapeutics. *Signal Transduct Target Ther* 7: 95, 2022.
- Wolfe MS, Xia W, Ostaszewski BL, Diehl TS, Kimberly WT and Selkoe DJ: Two transmembrane aspartates in presenilin-1 required for presenilin endoproteolysis and gamma-secretase activity. *Nature* 398: 513-517, 1999.
- Levitán D, Lee J, Song L, Manning R, Wong G, Parker E and Zhang L: PS1 N- and C-terminal fragments form a complex that functions in APP processing and Notch signaling. *Proc Natl Acad Sci USA* 98: 12186-12190, 2001.
- Güner G and Lichtenthaler SF: The substrate repertoire of  $\gamma$ -secretase/presenilin. *Semin Cell Dev Biol* 105: 27-42, 2020.
- Steinbuck MP and Winandy S: A review of Notch processing with new insights into ligand-independent Notch signaling in T-cells. *Front Immunol* 9: 1230, 2018.
- Hosokawa H and Rothenberg EV: How transcription factors drive choice of the T cell fate. *Nat Rev Immunol* 21: 162-176, 2021.
- Weng AP, Ferrando AA, Lee W, Morris JP IV, Silverman LB, Sanchez-Irizarry C, Blacklow SC, Look AT and Aster JC: Activating mutations of NOTCH1 in human T cell acute lymphoblastic leukemia. *Science* 306: 269-271, 2004.
- Sulis ML, Williams O, Palomero T, Tosello V, Pallikuppam S, Real PJ, Barnes K, Zuurbier L, Meijerink JP and Ferrando AA: NOTCH1 extracellular juxtamembrane expansion mutations in T-ALL. *Blood* 112: 733-740, 2008.
- Ferrando AA: The role of NOTCH1 signaling in T-ALL. *Hematology Am Soc Hematol Educ Program*: 353-361, 2009.
- Ashworth TD, Pear WS, Chiang MY, Blacklow SC, Mastio J, Xu L, Kelliher M, Kastner P, Chan S and Aster JC: Deletion-based mechanisms of Notch1 activation in T-ALL: Key roles for RAG recombinase and a conserved internal translational start site in Notch1. *Blood* 116: 5455-5464, 2010.
- Real PJ, Tosello V, Palomero T, Castillo M, Hernandez E, de Stanchina E, Sulis ML, Barnes K, Sawai C, Homminga I, *et al*: Gamma-secretase inhibitors reverse glucocorticoid resistance in T cell acute lymphoblastic leukemia. *Nat Med* 15: 50-58, 2009.

22. López-Nieva P, González-Sánchez L, Cobos-Fernández MÁ, Córdoba R, Santos J and Fernández-Piqueras J: More insights on the use of  $\gamma$ -secretase inhibitors in cancer treatment. *Oncologist* 26: e298-e305, 2021.
23. Baratta MG: Adjusting the focus on  $\gamma$ -secretase inhibition. *Nat Rev Cancer* 19: 419, 2019.
24. Habets RA, De Bock CE, Serneels L, Lodewijckx I, Verbeke D, Nittner D, Narlawar R, Demeyer S, Dooley J, Liston A, *et al.*: Safe targeting of T cell acute lymphoblastic leukemia by pathology-specific NOTCH inhibition. *Sci Transl Med* 11: eaau6246, 2019.
25. Palomero T, Sulis ML, Cortina M, Real PJ, Barnes K, Ciofani M, Caparros E, Buteau J, Brown K, Perkins SL, *et al.*: Mutational loss of PTEN induces resistance to NOTCH1 inhibition in T-cell leukemia. *Nat Med* 13: 1203-1210, 2007.
26. Martelli AM, Paganelli F, Fazio A, Bazzichetto C, Conciatori F and McCubrey JA: The key roles of PTEN in T-cell acute lymphoblastic leukemia development, progression, and therapeutic response. *Cancers (Basel)* 11: 629, 2019.
27. Gills JJ, Lopiccio J, Tsurutani J, Shoemaker RH, Best CJ, Abu-Asab MS, Borojerdi J, Warfel NA, Gardner ER, Danish M, *et al.*: Nelfinavir, A lead HIV protease inhibitor, is a broad-spectrum, anticancer agent that induces endoplasmic reticulum stress, autophagy, and apoptosis in vitro and in vivo. *Clin Cancer Res* 13: 5183-5194, 2007.
28. Blumenthal GM, Gills JJ, Ballas MS, Bernstein WB, Komiya T, Dechowdhury R, Morrow B, Root H, Chun G, Helsabeck C, *et al.*: A phase I trial of the HIV protease inhibitor nelfinavir in adults with solid tumors. *Oncotarget* 5: 8161-8172, 2014.
29. Kawabata S, Connis N, Gills JJ, Hann CL and Dennis PA: Nelfinavir inhibits the growth of small-cell lung cancer cells and patient-derived xenograft tumors. *Anticancer Res* 41: 91-99, 2021.
30. Subeha MR and Telleria CM: The anti-cancer properties of the HIV protease inhibitor Nelfinavir. *Cancers (Basel)* 12: 3437, 2020.
31. Eder J, Hommel U, Cumin F, Martoglio B and Gerhartz B: Aspartic proteases in drug discovery. *Curr Pharm Des* 13: 271-285, 2007.
32. Lobbardi R, Pinder J, Martinez-Pastor B, Theodorou M, Blackburn JS, Abraham BJ, Namiki Y, Mansour M, Abdelfattah NS, Molodtsov A, *et al.*: TOX regulates growth, DNA repair, and genomic instability in T-cell acute lymphoblastic leukemia. *Cancer Discov* 7: 1336-1353, 2017.
33. Kawabata S, Mercado-Matos JR, Hollander MC, Donahue D, Wilson W III, Regales L, Butaney M, Pao W, Wong KK, Jänne PA and Dennis PA: Rapamycin prevents the development and progression of mutant epidermal growth factor receptor lung tumors with the acquired resistance mutation T790M. *Cell Rep* 7: 1824-1832, 2014.
34. Farmery MR, Tjernberg LO, Pursglove SE, Bergman A, Winblad B and Näslund J: Partial purification and characterization of gamma-secretase from post-mortem human brain. *J Biol Chem* 278: 24277-24284, 2003.
35. Kim SK, Park HJ, Hong HS, Baik EJ, Jung MW and Mook-Jung I: ERK1/2 is an endogenous negative regulator of the gamma-secretase activity. *FASEB J* 20: 157-159, 2006.
36. Kawabata S, Hollander MC, Munasinghe JP, Brinster LR, Mercado-Matos JR, Li J, Regales L, Pao W, Jänne PA, Wong KK, *et al.*: Epidermal growth factor receptor as a novel molecular target for aggressive papillary tumors in the middle ear and temporal bone. *Oncotarget* 6: 11357-11368, 2015.
37. Bachhawat AK and Kaur A: Glutathione degradation. *Antioxid Redox Signal* 27: 1200-1216, 2017.
38. Chi Z, Byrne ST, Dolinko A, Harraz MM, Kim MS, Umanah G, Zhong J, Chen R, Zhang J, Xu J, *et al.*: Botch is a  $\gamma$ -glutamyl cyclotransferase that deglycinates and antagonizes Notch. *Cell Rep* 7: 681-688, 2014.
39. Lin YW, Nichols RA, Letterio JJ and Aplan PD: Notch1 mutations are important for leukemic transformation in murine models of precursor-T leukemia/lymphoma. *Blood* 107: 2540-2543, 2006.
40. Santos LO, Garcia-Gomes AS, Catanho M, Sodre CL, Santos ALS, Branquinha MH and d'Avila-Levy CM: Aspartic peptidases of human pathogenic trypanosomatids: Perspectives and trends for chemotherapy. *Curr Med Chem* 20: 3116-3133, 2013.
41. Gu Y, Wang X, Wang Y, Wang Y, Li J and Yu FX: Nelfinavir inhibits human DDI2 and potentiates cytotoxicity of proteasome inhibitors. *Cell Signal* 75: 109775, 2020.
42. De Strooper B, Iwatsubo T and Wolfe MS: Presenilins and  $\gamma$ -secretase: Structure, function, and role in Alzheimer disease. *Cold Spring Harb Perspect Med* 2: a006304, 2012.
43. Li X, Dang S, Yan C, Gong X, Wang J and Shi Y: Structure of a presenilin family intramembrane aspartate protease. *Nature* 493: 56-61, 2013.
44. Fukumori A, Fluhner R, Steiner H and Haass C: Three-amino acid spacing of presenilin endoproteolysis suggests a general stepwise cleavage of gamma-secretase-mediated intramembrane proteolysis. *J Neurosci* 30: 7853-7862, 2010.
45. Gertsik N, Ballard TE, Am Ende CW, Johnson DS and Li YM: Development of CBAP-BPpyne, a probe for  $\gamma$ -secretase and presenilinase. *Medchemcomm* 5: 338-341, 2014.
46. Sato T, Diehl TS, Narayanan S, Funamoto S, Ihara Y, De Strooper B, Steiner H, Haass C and Wolfe MS: Active gamma-secretase complexes contain only one of each component. *J Biol Chem* 282: 33985-33993, 2007.
47. Rand MD, Grimm LM, Artavanis-Tsakonas S, Patriub V, Blacklow SC, Sklar J and Aster JC: Calcium depletion dissociates and activates heterodimeric notch receptors. *Mol Cell Biol* 20: 1825-1835, 2000.
48. Meckler X and Checler F: Presenilin 1 and presenilin 2 target  $\gamma$ -secretase complexes to distinct cellular compartments. *J Biol Chem* 291: 12821-12837, 2016.
49. Stanga S, Vranx C, Tasiaux B, Marinangeli C, Karlström H and Kienlen-Campard P: Specificity of presenilin-1- and presenilin-2-dependent  $\gamma$ -secretases towards substrate processing. *J Cell Mol Med* 22: 823-833, 2018.
50. Mungrue IN, Pagnon J, Kohannim O, Gargalovic PS and Lusic AJ: CHAC1/MGC4504 is a novel proapoptotic component of the ATF4-ATF3-CHOP cascade. *J Immunol* 182: 466-476, 2009.
51. Kumar A, Tikoo S, Maity S, Sengupta S, Sengupta S, Kaur A and Bachhawat AK: Mammalian proapoptotic factor ChaC1 and its homologues function as  $\gamma$ -glutamyl cyclotransferases acting specifically on glutathione. *EMBO Rep* 13: 1095-1101, 2012.
52. Chi Z, Zhang J, Tokunaga A, Harraz MM, Byrne ST, Dolinko A, Xu J, Blackshaw S, Gaiano N, Dawson TM and Dawson VL: Botch promotes neurogenesis by antagonizing Notch. *Dev Cell* 22: 707-720, 2012.
53. Sathe A, Chalaud G, Oppolzer I, Wong KY, von Busch M, Schmid SC, Tong Z, Retz M, Gschwend JE, Schulz WA and Nawroth R: Parallel PI3K, AKT and mTOR inhibition is required to control feedback loops that limit tumor therapy. *PLoS One* 13: e0190854, 2018.
54. Yang M, Lu Y, Piao W and Jin H: The translational regulation in mTOR pathway. *Biomolecules* 12: 802, 2022.
55. Budanov AV, Shoshani T, Faerman A, Zelin E, Kamer I, Kalinski H, Gorodin S, Fishman A, Chajut A, Einat P, *et al.*: Identification of a novel stress-responsive gene Hi95 involved in regulation of cell viability. *Oncogene* 21: 6017-6031, 2002.
56. Velasco-Miguel S, Buckbinder L, Jean P, Gelbert L, Talbott R, Laidlaw J, Seizinger B and Kley N: PA26, a novel target of the p53 tumor suppressor and member of the GADD family of DNA damage and growth arrest inducible genes. *Oncogene* 18: 127-137, 1999.
57. Peeters H, Debeer P, Bairoch A, Wilquet V, Huysmans C, Parthoens E, Fryns JP, Gewillig M, Nakamura Y, Niikawa N, *et al.*: PA26 is a candidate gene for heterotaxia in humans: Identification of a novel PA26-related gene family in human and mouse. *Hum Genet* 112: 573-580, 2003.
58. Saveljeva S, Cleary P, Mnich K, Ayo A, Pakos-Zebrucka K, Patterson JB, Logue SE and Samali A: Endoplasmic reticulum stress-mediated induction of SESTRIN 2 potentiates cell survival. *Oncotarget* 7: 12254-12266, 2016.
59. Lee JH, Cho US and Karin M: Sestrin regulation of TORC1: Is sestrin a leucine sensor? *Sci Signal* 9: re5, 2016.
60. Brüning A, Rahmeh M and Friese K: Nelfinavir and bortezomib inhibit mTOR activity via ATF4-mediated sestrin-2 regulation. *Mol Oncol* 7: 1012-1018, 2013.
61. Hales EC, Taub JW and Matherly LH: New insights into Notch1 regulation of the PI3K-AKT-mTOR1 signaling axis: Targeted therapy of  $\gamma$ -secretase inhibitor resistant T-cell acute lymphoblastic leukemia. *Cell Signal* 26: 149-161, 2014.
62. Shen W, Zhou Q, Peng C, Li J, Yuan Q, Zhu H, Zhao M, Jiang X, Liu W and Ren C: FBXW7 and the hallmarks of cancer: Underlying mechanisms and prospective strategies. *Front Oncol* 12: 880077, 2022.

